Clinical Stages of Occult Macular Dystrophy Based on Optical Coherence Tomographic Findings

Natsuko Nakamura,[1,2] Kazushige Tsunoda,[1] Yoshinobu Mizuno,[3] Tomoaki Usui,[4] Tetsuhisa Hatase,[5] Shinji Ueno,[6] Kazuki Kuniyoshi,[7] Takaaki Hayashi,[8] Satoshi Katagiri,[8] Mineo Kondo,[9] Shuhei Kameya,[10] Kazutoshi Yoshitake,[11] Kaoru Fujinami,[1,12,13] Takeshi Iwata,[11] and Yozo Miyake[1,14]

[1]Division of Vision Research, National Institute of Sensory Organs, National Hospital Organization Tokyo Medical Center, Tokyo, Japan
[2]Department of Ophthalmology, The University of Tokyo, Tokyo, Japan
[3]Department of Ophthalmology, Teikyo University, Tokyo, Japan
[4]Akiba Eye Clinic, Niigata, Japan
[5]Division of Ophthalmology and Visual Science, Graduate School of Medical and Dental Sciences, Niigata University, Niigata, Japan
[6]Department of Ophthalmology, Nagoya University Graduate School of Medicine, Nagoya, Aichi, Japan
[7]Department of Ophthalmology, Kindai University Faculty of Medicine, Osaka-Sayama, Osaka, Japan
[8]Department of Ophthalmology, The Jikei University School of Medicine, Tokyo, Japan
[9]Department of Ophthalmology, Mie University Graduate School of Medicine, Tsu, Mie, Japan
[10]Department of Ophthalmology, Nippon Medical School Chiba Hokusoh Hospital, Inzai, Chiba, Japan
[11]Division of Molecular and Cellular Biology, National Institute of Sensory Organs, National Hospital Organization Tokyo Medical Center, Tokyo, Japan
[12]University College London Institute of Ophthalmology, London, United Kingdom
[13]Department of Ophthalmology, Keio University School of Medicine, Tokyo, Japan
[14]Kobe Eye Center, Hyogo, Japan

Correspondence: Kazushige Tsunoda, Division of Vision Research, National Institute of Sensory Organs, National Hospital Organization Tokyo Medical Center, 2-5-1 Higashigaoka, Meguro-ku, Tokyo 152-8902, Japan; tsunodakazushige@kankakuki.go.jp.

Submitted: May 9, 2019
Accepted: October 9, 2019

Citation: Nakamura N, Tsunoda K, Mizuno Y, et al. Clinical stages of occult macular dystrophy based on optical coherence tomographic findings. *Invest Ophthalmol Vis Sci*. 2019;60:4691–4700. https://doi.org/10.1167/iovs.19-27486

Purpose. To determine the course of occult macular dystrophy (OMD, Miyake's disease) and to propose stages of OMD based on the optical coherence tomographic (OCT) findings.

Methods. Sixty-one patients from 33 families with OMD who carried one of the proven variants of the *RP1L1* gene were studied at seven centers in Japan. Ophthalmological examinations including the best-corrected visual acuity (BVCA) and OCT were performed.

Results. The median age at the last visit was 50 years with a range of 10 to 88 years, and the median age at the symptom onset was 30 years with a range of 3 to 60 years. There were significant negative correlations between the duration of OMD and BCVA, the central retinal thickness (CRT) and the thickness between external limiting membrane and retinal pigment epithelium (ERT). The BCVA gradually decreased for 10 years after symptom onset and was stable thereafter. Kaplan-Meier survival curves of the BCVA and retinal thickness showed that all of the patients had retained a vision of 1.0 logMAR, and over 80% of the patients had retained 50% thickness of the normal CRT and ERT for at least 60 years after symptom onset. The stages of OMD based on the visual symptoms and OCT findings are proposed.

Conclusions. The photoreceptors do not become completely atrophic even at the late stage, which may account for the good retinal pigment epithelium (RPE) structure and normal-appearing fundus. The proposed stages facilitate the investigation of the pathogenicity of OMD and provide information to determine the effectiveness of therapeutic procedures.

Keywords: occult macular dystrophy, *RP1L1*, OCT, staging, Miyake's disease

Occult macular dystrophy (OMD; Online Mendelian Inheritance in Man [OMIM] 613587) is a dominantly inherited macular dystrophy that is characterized by normal-appearing fundus and normal fluorescein angiograms during the entire course of the disease process.[1–3] Since the retinitis pigmentosa 1-like 1 (*RP1L1*) gene (OMIM 608581) was identified as one of the causative genes of OMD,[4,5] a number of *RP1L1* variants have been reported to be associated with OMD.[6–12] The most common variant is the c.133C>T, p.Arg45Trp mutation in exon 2, and there is another hot spot between amino acid numbers 1194 and 1201 in exon 4.[10,11] In a multicenter study of a Japanese cohort with OMD, the patients having the *RP1L1* gene mutations were found to have common findings in optical coherence tomographic (OCT) images, and this classical phenotype was named Miyake's disease.[11]

Recently, a number of therapeutic procedures have been developed for various types of inherited retinal diseases. Although the pathogenic mechanism(s) has not been determined for OMD, information on the natural course and establishing clinical stages are crucial for determining the

effectiveness of the different therapeutic procedures and in selecting appropriate candidates for the treatments.[13,14] The OCT findings play an important role in the diagnosis of OMD.[5,11,15,16] In an earlier report of a large family having the *RP1L1* gene mutation (p.Arg45Trp), Tsunoda et al.[5] documented that the photoreceptor structures, assessed by OCT, gradually changed during the course of OMD.

To investigate the natural course and clinical stages of OMD, we have determined the association between age, duration of the disease, visual acuity, and the retinal structures determined by OCT in 61 patients with *RP1L1* gene mutations.

The aim of this study was to determine the course of OMD. This was a multicenter study of 61 patients of 33 families with OMD. We shall propose the clinical stages of OMD based on the visual symptoms and OCT findings.

Patients and Methods

The procedures used in this study adhered to the tenets of the Declaration of Helsinki and were approved by the Ethics Committee of the participating institutions: National Institute of Sensory Organs, National Hospital Organization Tokyo Medical Center (Reference; R18-029), Niigata University, Nagoya University, Kinki University, Jikei University, Mie University, and Nippon Medical School Chiba Hokusoh Hospital. An informed consent was received from all of the subjects for the examinations used in this study after an explanation of the nature and possible consequences of the study.

Participants

We studied 61 patients (33 families) with OMD who carried one of the known proven variants in the two hot spots of the *RP1L1* gene, a missense mutation in amino acid number 45 in exon 2, and in amino acid numbers 1194 to 1201 in exon 4, from the phenotype–genotype database of the Japan Eye Genetics Consortium (JEGC) (Table 1).

The classical signs and symptoms of OMD were a progressive decrease of the visual acuity in both eyes, essentially normal funduscopic appearance, normal full-field ERGs, and localized macular dysfunction detected by focal macular or multifocal electroretinograms (ERGs).[1–3] However, five asymptomatic family members who had abnormalities both in the OCT images and in the *RP1L1* gene were included for the establishment of the stages of OMD.[16] Some of the clinical and genetic data have been published elsewhere.[5,11,16,17]

Clinical Investigations

A detailed medical history was obtained from all the patients including the visual symptoms and the onset of disease, that is, when the visual symptoms were first noted or when OMD was first diagnosed. Complete ophthalmic examinations were performed including measurements of the decimal best-corrected visual acuity (BCVA), ophthalmoscopy, fundus photography, and spectral-domain OCT. The decimal BCVA was converted to logarithm of the minimum angle of resolution (logMAR) units, and only data of the right eye were used for the statistical analyses.

OCT Analyses

The spectral-domain OCT images of high-resolution line scans were obtained from 58 patients (Cirrus HD-OCT; Carl Zeiss Meditec, Dublin, CA, USA, or Spectralis; Heidelberg Engineering, Heidelberg, Germany). For the quantitative analyses of the retinal thickness, only the data from the Cirrus OCT device were used, and the eyes with ocular conditions that can influence the measurements of the retinal thicknesses, for example, glaucoma, epiretinal membrane, and significant refractive errors (hyperopia $> +2.0$ diopter or myopia < -6.0 diopter), were excluded. The data of only the right eye were used for the statistical analyses. When the right eye was not available due to an exclusion criterion, the data of the left eye were used for the statistical analyses. In the end, data from 42 eyes were used for the OCT measurements (14 men and 28 women; age, 13 to 88 years, median age, 54.5 years). The retinal thicknesses were also measured from 55 control eyes (16 men and 39 women; age, 18 to 71 years, median age, 42.0 years). There was no significant difference in the refractive errors between OMD and the controls. The mean $\pm$ SD of the refractive error (spherical equivalent) was -1.83 ± 2.08 in OMD and -1.50 ± 1.95 in controls ($P = 0.24$, Mann-Whitney U tests).

The retinal thickness was measured manually by the built-in scale of the SD-OCT system by two experienced ophthalmologists (N.N. and K.T.) independently, and the average of the two measurements was used for the statistical analyses. The central retinal thickness (CRT) was defined as the distance between the inner retinal surface and inner margin of the retinal pigment epithelium (RPE) at the foveola. To evaluate the length of photoreceptor outer segment, we measured the distance between the external limiting membrane (ELM) and inner margin of the RPE at the foveola, and this distance was defined as the ELM-RPE thickness (ERT). We were not able to use the ellipsoid zone (EZ) as a landmark of the photoreceptors because the border of EZ was significantly blurred and difficult to identify in most of the cases with OMD.

Stages of OMD

The clinical stages were determined by the presence of visual symptoms and by the microstructures of the photoreceptors detected by the OCT in 58 patients. The microstructures of the fovea were graded independently by two experienced ophthalmologists (N.N. and K.T.). During this procedure, all of the patients' information, including the BCVA and duration of the disease, was masked to the examiners. In cases where the gradings were different, discussions were held by looking at other line-scan images until both examiners reached a common grading.

The staging was based on the rationale that patients with symptoms should be at a more advanced stage than those without, and that patients with severely damaged photoreceptor structures in the OCT images should be at a more advanced stage than those with less severe damage. Second, we have shown in an earlier study that the photoreceptor structures observed in the OCT images varied according to the duration of OMD, and that abnormalities in both the interdigitation zone (IZ) and EZ in the macular region were vulnerable OCT markers for the duration of OMD in patients with the *RP1L1* gene mutations.[5] The characteristics of the individual markers observed in the patients with different disease durations are presented in Table 2. In our cohort, all the patients could be categorized into one of three stages: stage I (Ia and Ib), stage II (IIa and IIb), and stage III (IIIa and IIIb).

The IZ at the fovea in the OCT images was graded into two categories: normal or extinguished. The foveal bulge of the EZ, which appeared as a small arc-like protrusion in normal eyes, was graded into two categories: present or absent. The EZ at the fovea was graded into three categories: normal, blurred, or disrupted. The clinical stages were determined by considering

Investigative Ophthalmology & Visual Science

Table 1. Summary of Clinical Characteristics and *RP1L1* Variants in 61 Patients

Patient No.	Patient ID	Sex	*RP1L1* Variants	Age at Symptom Onset, y	Age at Last Visit, y	Duration From Symptom Onset to Last Visit, y	Visual Symptoms		Decimal BCVA at Last Visit	
							1st	2nd	OD	OS
1	KA-003	M	S1199C	47	60	13	Reduced VA	Photophobia	0.2	0.1
2	KA-004	F	S1199C	20	88	68	Reduced VA		0.2	0.07
3	KA-006	F	S1199C	60	82	22	Photophobia	Reduced VA	0.1	0.1
4	KA-007	F	G1200D	50	76	26	Reduced VA	Photophobia	0.1	0.1
5	KA-010	F	G1200A	40	54	14	Reduced VA	Photophobia	0.1	0.2
6	KA-011	M	S1199C	37	49	12	Reduced VA	Photophobia	0.3	0.3
7	KA-013	F	R45W	14	75	61	Reduced VA	Photophobia	0.1	0.08
8	KA-014	F	R45W	18	35	17	Reduced VA	Photophobia	0.2	0.2
9	KA-017	F	R45W	38	48	10	Reduced VA	Photophobia	0.1	0.1
10	KA-018	M	T1194M / T1196I	45	52	7	Reduced VA	Photophobia	0.3	0.2
11	KA-035	F	R45W	25	34	9	Reduced VA	Photophobia	0.2	0.2
12	KA-067	F	R45W	7	19	12	Reduced VA	Photophobia	0.15	0.15
13	KA-068	F	R45W	40	50	10	Photophobia	Reduced VA	0.1	0.1
14	KA-071	M	V1201G	25	50	25	Reduced VA	Photophobia	0.15	0.15
15	KA-208	M	S1199C	26	34	8	Reduced VA	Photophobia	0.4	0.3
16	KA-209	F	S1199C	No symptoms	65	0	None		1.2	1.2
17	KA-235	F	S1199C	50	66	16	Photophobia	Reduced VA	0.15	0.15
18	KA-243	F	G1200D	No symptoms	52	0	None		1.0	1.0
19	KA-290	F	R45W	11	21	10	Reduced VA	Photophobia	0.1	0.1
20	KA-291	F	R45W	No symptoms	50	0	None		1.0	1.2
21	KA-292	M	S1199C	33	38	5	Reduced VA		0.4	0.15
22	KA-293	M	S1199C	13	37	24	Reduced VA	Photophobia	0.5	0.5
23	KA-305	F	R45W	21	70	49	Reduced VA	Photophobia	0.1	0.1
24	KA-311	F	S1199C	60	69	9	Reduced VA	Photophobia	0.4	0.3
25	KA-312	F	S1199C	30	45	15	Reduced VA	Photophobia	0.3	0.2
26	KA-313	F	R45W	37	55	18	Reduced VA	Photophobia	0.1	0.1
27	KA-345	M	R45W	40	48	8	Reduced VA	Photophobia	0.3	0.2
28	SMOP-N01	F	R45W	No symptoms	49	0	None		1.5	1.5
29	SMOP-N03	M	R45W	30	74	44	Reduced VA	Photophobia	0.2	0.3
30	SMOP-N08	F	R45W	50, OS	81	31	OS: Reduced VA OD: None		1.2	0.1
31	SMOP-P01	F	R45W	40	57	17	Reduced VA		0.1	0.4
32	SMOP-P02	F	R45W	10	58	48	Reduced VA		0.2	0.15
33	SMOP-P03	F	R45W	6	18	12	Reduced VA		0.15	0.15
34	SMOP-P06	M	R45W	20	83	63	Reduced VA		0.15	0.15
35	SMOP-P07	M	R45W	13	21	8	Reduced VA		0.3	0.3
36	SMOP-P08	M	R45W	30	66	36	Reduced VA		0.2	0.3
37	SMOP-P09	F	R45W	25	71	46	Reduced VA	Photophobia	0.3	0.3
38	SMOP-P11	M	R45W	18	70	52	Reduced VA	Photophobia	0.2	0.15
39	SMOP-P12	F	R45W	40	69	29	Reduced VA	Photophobia	0.1	0.08
40	KINKI-002-2	F	R45W	28	43	15	Reduced VA		0.3	0.4
41	KINKI-030-11	M	R45W	60	70	10	Reduced VA		0.1	0.2
42	KINKI-030-14	M	R45W	58	62	4	Reduced VA		0.15	0.15
43	KINKI-070-0017	F	R45W	19	25	6	Reduced VA	Color vision abnormality	0.2	0.2
44	KINKI-070-0018	F	R45W	12	52	40	Reduced VA		0.1	0.15
45	KINKI-070-0019	M	R45W	8	15	7	Reduced VA		0.2	0.2
46	Nagoya-003-0003	F	R45W	42	52	10	Reduced VA		0.3	0.6
47	Nagoya-006-0006	M	G1200V	40	62	22	Reduced VA		0.5	0.3
48	Nagoya-007-0007	M	R45W	20	49	29	Reduced VA		0.16	0.16
49	Nagoya-040-0040	F	R45W	39	48	9	Reduced VA		0.2	0.2
50	Nagoya-144-0144	F	R45W	38	40	2	Photophobia	Reduced VA	0.4	0.5
51	Nagoya-144-1144	M	R45W	3	12	9	Reduced VA		0.1	0.1
52	Nagoya-157-0157	F	R45W	20	49	29	Photophobia	Reduced VA	0.3	0.25
53	Nagoya-157-1157	M	R45W	8	10	2	Reduced VA		0.7	0.6
54	MIEU-069-0093	M	R45W	37	47	10	Reduced VA		0.6	0.7
55	MIEU-072-0096	F	R45W	41	42	1	Reduced VA		1	0.4
56	JIKEI-228-JU1409	M	R45W	41	47	6	Reduced VA		0.2	0.2
57	JIKEI-253-JU0409	M	S1199C	35	50	15	Reduced VA		0.3	0.2
58	JIKEI-253-JU0484	M	S1199C	17	83	66	Reduced VA		0.15	0.15
59	JIKEI-254-JU0089	F	R45W	33	70	37	Reduced VA		0.3	0.2
60	JIKEI-254-JU0090	F	R45W	21	43	22	Reduced VA		0.4	0.4
61	NMSCHH-008-01	F	S1199C	50	57	7	Reduced VA		0.2	0.2

OD, right eye; OS, left eye; VA, visual acuity.

Table 2. Characteristics of OCT Markers in the Macula for Different Disease Durations of the Cases With *RP1L1* Gene Mutations

OCT Markers in the Macula	Short Duration	←	→	Long Duration
IZ: normal (+) or extinguished (−)	+	−	−	−
Foveal bulge: present (+) or absent(−)	+	+	−	−
EZ: normal (+), blurred (±), or disrupted (−)	+	±	±	−
Stages	Ia or Ib*	IIa or IIb†	IIIa	IIIb

* Asymptomatic cases with minimal abnormality of IZ and EZ only at the foveal center were categorized as Ia, and those with minimal abnormality only at the parafovea were categorized as Ib.

† Symptomatic cases with abnormality of IZ and EZ only at the fovea were categorized as IIa, and those with abnormality at the entire macula were categorized as IIb.

both the presence of visual symptoms and the severity of these three markers in the OCT images (Table 2).

The clinical stages were stage I, no visual symptoms and minimal structural changes in the OCT images; stage II, IZ not present and EZ blurred and dome-shaped; and stage III, EZ appeared flat (Table 2; Fig. 1). Stage I was further subdivided into stages Ia and Ib: Stage Ia, only minimal structural changes are present at the foveal center, and stage Ib, only the parafoveal structures are altered. Stage II was also subdivided into two substages: Stage IIa, only the foveal region was impaired; and stage IIb, the entire macular region was impaired. Stage III was subdivided into two substages: Stage IIIa, the EZ is continuous; and stage IIIb, the EZ is disrupted at the fovea.

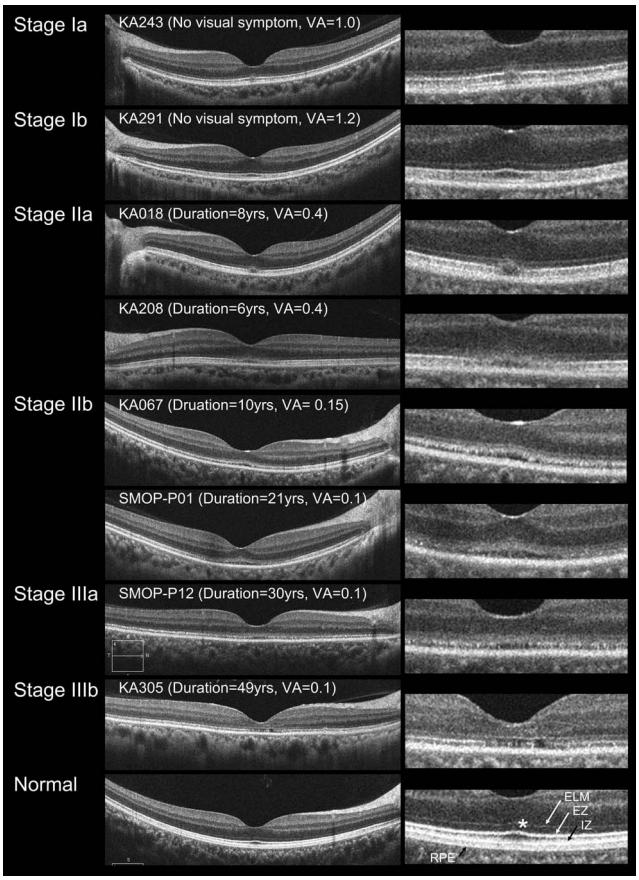

Figure 1. Optical coherence tomographic images showing a horizontal profile of the retina along the foveola (*left*) and magnified images of the foveal region (*right*) for different stages of OMD patients and a normal control. Representative OCT images of one or two patients for each stage are presented with disease duration and BCVA. The outer retinal structures, for example, the ELM, EZ, IZ, and RPE, are indicated by the *arrows*. The foveal bulge is indicated by an *asterisk*. VA, visual acuity.

Statistical Analyses

The statistical analyses were performed with IBM SPSS Statistics 24.0 (IBM, Armonk, NY, USA). Spearman's rank-order correlations were calculated to identify the significance of the correlations between BCVA and age, BCVA and the duration of OMD, retinal thickness and age, retinal thickness and duration of OMD, and retinal thickness and the BCVA. Mann-Whitney *U* tests were used to determine the significance of the differences in the retinal thickness between patients and controls. Steel-Dwass tests were used to compare the disease duration, BCVA, CRT, and ERT among the three stages. P values < 0.05 were considered statistically significant.

Results

Clinical and Genetic Findings of the Cohorts

Detailed demographics of the age at the onset of the visual symptoms, kinds of symptoms, BCVA, and type of variant of the *RP1L1* gene for all the patients are presented in Table 1. There were 37 women and 24 men. All of the patients had heterozygous proven variants in one of the two hot spots of the *RP1L1* gene.[11] The type of variants included R45W in 41 patients, S1199C in 14 patients, G1200D in 2 patients, and one each of G1200A, G1200V, V1201G, and T1194M/T1196I (complex). The median age at the last visit was 50 years with a range of 10 to 88 years (mean ± SD, 51.9 ± 18.8 years), and the median age at the onset of symptoms was 30 years with a range of 3 to 60 years (mean ± SD; 30.5 ± 15.1 years). The median interval from symptom onset to last visit was 13.0 years with a range of 0 to 68 years (mean ± SD; 19.9 ± 17.9 years).

Fifty-two patients (52/61, 85.2%) complained of reduced BCVA as the initial symptom, and 57 patients (57/61, 93.4%) complained of reduced BCVA during the course of the study. Only 5 patients (5/61, 8.2%) complained of photophobia as the initial symptom; however, 23 patients complained of photophobia at a time later than the reduction of the BCVA. In total, 28 patients (28/61, 45.9%) complained of photophobia during the course of the study. There were eight eyes of four patients and one eye of one patient that did not have any visual symptoms, and the abnormalities of these eyes were unexpectedly detected by OCT when they were examined as unaffected family members.

Relationship Between BCVA and Age and Duration of OMD

The decimal BCVA ranged from 0.1 to 1.5 or 1.0 to −0.176 logMAR units with a mean ± SD of 0.62 ± 0.32 logMAR unit in the right eye. Scatter plots of the BCVAs as a function of the age

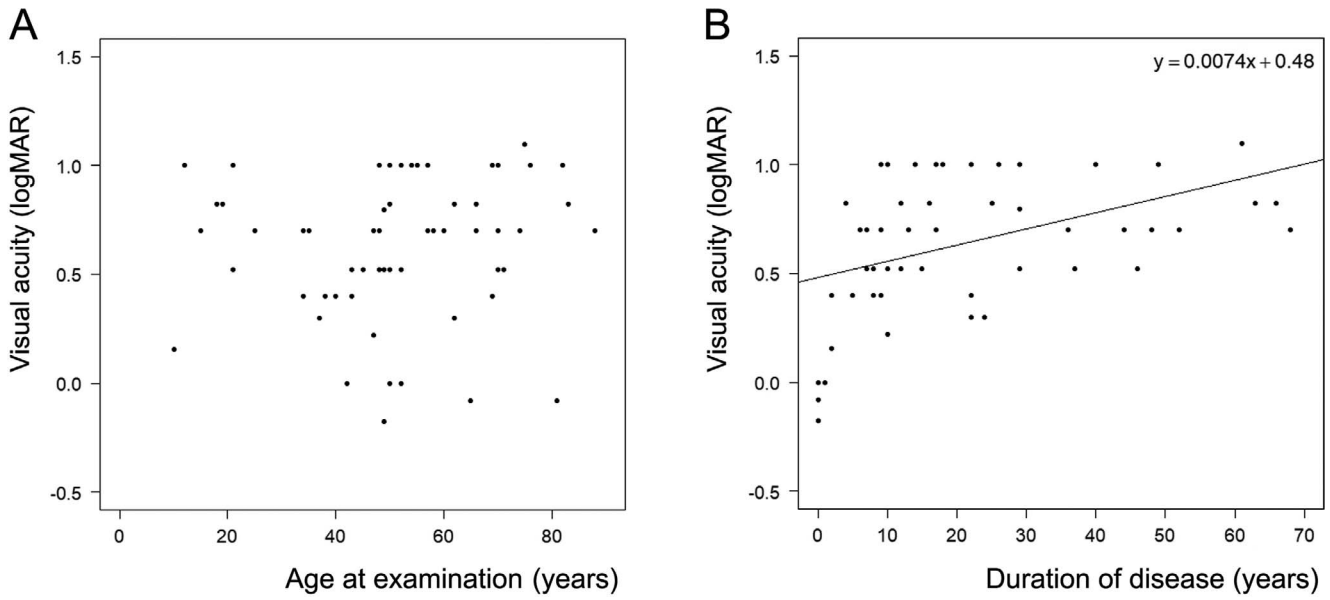

FIGURE 2. Scatter plots of BCVA in logMAR units as a function of age at the time of the examination (**A**) and the years of disease duration (**B**). There was no significant correlation between the BCVA and age ($r = 0.234$, $P = 0.069$, Spearman's rank-order correlation) (**A**), but a significant correlation was present between the BCVA and years of disease duration ($r = 0.483$, $P < 0.001$) (**B**).

at the time of the examination and the duration of OMD are presented in Figure 2. There was no significant correlation between the BCVA and age ($r = 0.234$, $P = 0.069$, Spearman's rank-order correlation; Fig. 2A). However, a significant correlation was found between BCVA and the duration of the disease ($r = 0.483$, $P < 0.001$; Fig. 2B). In most of the patients, the BCVA did not worsen to 1.0 logMAR units during the course of this study.

Longitudinal Changes of Visual Acuity

Twenty-nine patients were followed in the same institutions for over 5 years, and the median follow-up period was 8.0 years with a range of 5 to 21 years. The BCVA at the initial examination and at the last visit are plotted as a function of the duration from the onset of symptoms to show the longitudinal changes during this period for the 29 patients (Fig. 3).

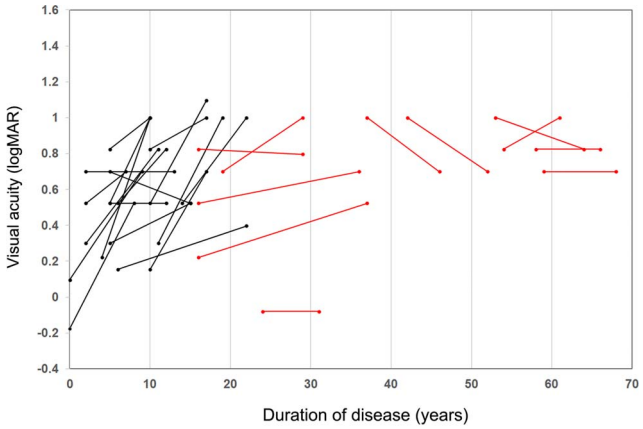

FIGURE 3. Longitudinal changes of the BCVA (logMAR units) for 29 patients. The BCVAs are plotted as a function of the duration from the onset of symptoms. The data of the patients whose initial visit was within 15 years after the onset of symptoms are indicated by the *black symbols*, and those whose initial visit was later than 15 years after the onset of symptoms are indicated by the *red symbols*.

For the patients whose initial visit was within 15 years after symptom onset, the visual acuity gradually deteriorated (black bars in Fig. 3). On the other hand, for those whose initial visit was later than 15 years after the onset of the symptoms, the visual acuity did not change significantly with increasing time (red bars in Fig. 3).

Central Retinal Thickness and ELM-RPE Thickness at the Fovea

The CRT and ERT were measured at the foveola of 42 patients and 55 control eyes. In the controls, the CRT was 202.0 ± 15.8 μm and the ERT was 88.0 ± 4.1. In the OMD patients, the CRT was 144.5 ± 31.2 μm and the ERT was 57.8 ± 9.4. Both were significantly thinner in the OMD eyes than in the controls ($P < 0.01$ for both; Mann–Whitney U tests).

In the OMD eyes, the correlations between age at the time of the examination and the CRT ($r = -0.233$, $P = 0.137$, Spearman's rank-order correlation) and ERT ($r = -0.148$, $P = 0.349$) were not significant. However, the correlations between the duration of OMD and CRT ($r = -0.616$, $P < 0.001$; Fig. 4A) and the ERT ($r = -0.437$, $P = 0.004$; Fig. 4B) were both significant. The correlations between CRT and BCVA ($r = -0.396$, $P < 0.01$; Fig. 4C), and between ERT and BCVA ($r = -0.328$, $P < 0.05$; Fig. 4D) were both significant.

Survival Curves of Visual Acuity, CRT, and ERT

To estimate the changes in the BCVA during the course of the disease, Kaplan-Meier survival curves were plotted with two cutoff points: loss of 0.52 logMAR unit (0.3 decimal unit) and loss of 1.0 in logMAR units (0.1 decimal unit; Fig. 5A). The survival curves demonstrated that the duration when the BCVA of one-half of the subjects reached 0.52 logMAR unit was 16 years. However, 100% of the patients were predicted to retain vision of at least 1.0 logMAR unit for at least 60 years after the onset of symptoms.

For CRT and ERT, the Kaplan-Meier survival curves for the duration of disease were plotted by using two cutoff points: reduction to less than 75% of the average thicknesses of normal

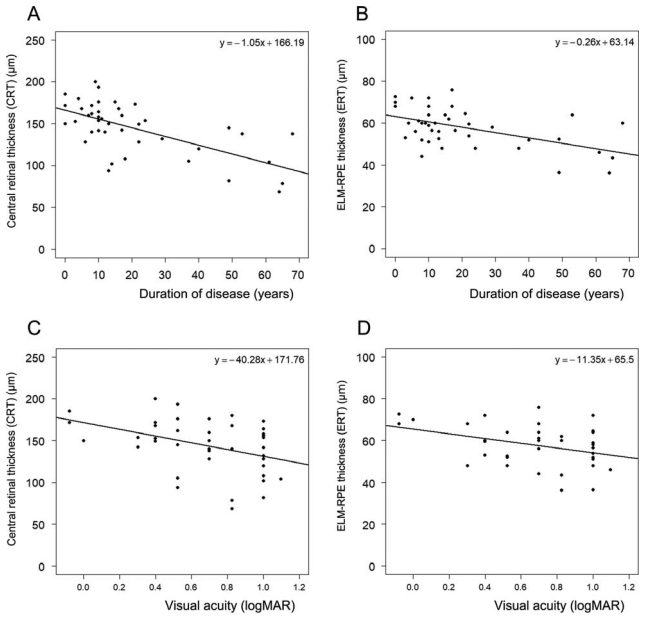

Figure 4. Scatter plot of CRT and ERT at the foveola as a function of the duration of OMD (**A**, **B**) and the visual acuity (**C**, **D**). Significant negative correlations were found between the disease duration and CRT ($r = -0.616$, $P < 0.001$, Spearman's rank-order correlation) (**A**) and disease duration and ERT ($r = -0.437$, $P = 0.004$) (**B**). Significant negative correlations were found between the visual acuity and CRT ($r = -0.396$, $P < 0.01$) (**C**) and visual acuity and ERT ($r = -0.328$, $P < 0.05$) (**D**).

eyes (151.5 μm for CRT and 66 μm for ERT; Figs. 5B, 5C) and a reduction to less than 50% of the normal average thickness (101 μm for CRT and 44 μm for ERT; Figs. 5B, 5C). The survival curves showed that the duration when one-half of the subjects would have 75% of the normal average CRT was 29 years. However, over 80% of the patients were predicted to retain 50% thickness of normal CRT until 60 years after the onset of the symptoms. Similarly, the duration when one-half of the subjects would have 75% of the normal average of ERT was 16 years. However, over 80% of the patients were predicted to retain 50% of the thickness of normal ERT until 60 years after the onset of the symptoms.

Clinical Stages of OMD

The photoreceptor structures at the fovea and parafoveal region determined by OCT gradually changed as the duration of OMD increased (Fig. 1).[5] We graded the OCT changes of the photoreceptor layers in 58 cases that are listed in the order of disease duration in Table 3 according to the criteria described in Methods (Table 2). All of the patients at stage I were asymptomatic and had good visual acuities. Stage II was the largest group among the OMD participants; the disease duration in stage IIa ranged from 3 to 8 years, and that of stage IIb ranged from 1 to 53 years. The decimal BCVA at stage II varied greatly from 0.1 to 1.0 logMAR units. Stage III was the late stage of OMD; the disease duration of stage IIIa ranged from 6 to 65 years, and that of stage IIIb ranged from 49 to 67 years. The decimal BCVA of the stage III patients ranged from 0.08 to 0.3 logMAR unit (Table 3).

Discussion

To the best of our knowledge, this is the largest number of OMD cases that have been studied.

One of the characteristics of OMD was that the duration after the symptom onset was significantly correlated with the BCVA but the age at the time of the examination was not (Fig. 2). This was probably because the age at symptom onset varied from 3 to 60 years. Another important characteristic was that the BCVA decreased gradually during a period of 10 to 15 years after the symptom onset, but then remained stable (Fig. 3). Similarly, over 90% of the patients could be predicted to retain their decimal BCVA of ≥0.1 for at least 60 years after the symptom onset (Fig. 5A). These results indicate the typical changes in the BCVA during the course of OMD; the decimal BCVA gradually decreased to approximately 0.3 in 10 to 15 years after the onset. The decimal BCVA later became stable and, in most cases, did not become worse than 0.1 thereafter.

Similar to the BCVA, the changes in CRT and ERT were significantly correlated with the duration of disease but not with the age at the time of the examination (Fig. 4). The survival curves demonstrated that the duration when one-half

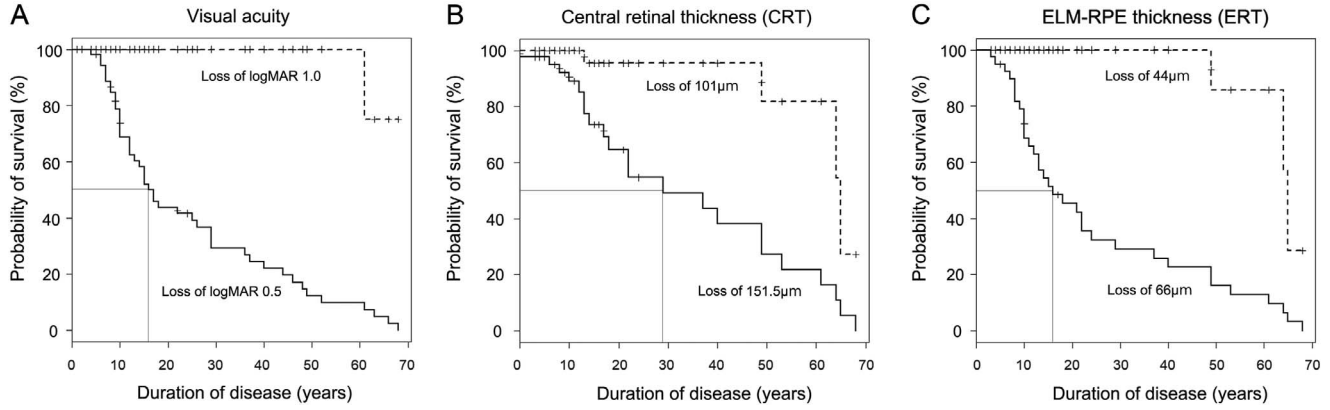

Figure 5. Kaplan-Meier survival curves of BCVA and retinal thickness as a function of the duration of the disease. For BCVA, two cutoff points were used: a loss of 0.52 logMAR unit (0.3 decimal unit) and a loss of 1.0 logMAR unit (0.1 decimal unit) (**A**). The survival curves would predict that 100% of the patients will retain vision of 1.0 logMAR unit for 60 years after the onset of symptoms. For both the CRT and ERT at the foveola, two cutoff points were used: a reduction to less than 75% of the normal average thickness (151.5 μm for CRT and 66 μm for ERT) and a reduction to less than 50% of the normal average thickness (101 μm for CRT and 44 μm for ERT) (**B**, **C**). The survival curves would predict that over 80% of the patients will retain 50% of the normal CRT until 60 years after the onset of symptoms (**B**), and would predict that over 80% of the patients will retain 50% thickness of normal ERT for 60 years after symptom onset (**C**).

Investigative Ophthalmology & Visual Science

Table 3. Staging of Occult Macular Dystrophy Based on Visual Symptoms and Findings of Optical Coherence Tomography

Patient No.	Duration From Symptom Onset, y	Decimal BCVA	IZ at the Fovea, Normal or Extinguished	EZ at the Fovea, Normal, Blurred, or Disrupted	Foveal Bulge of EZ, Present or Absent	Stage					
						Ia	Ib	IIa	IIb	IIIa	IIIb
16	0	1.2	Normal*	Normal†	Present		✓				
18	0	1.0	Extinguished‡	Blurred§	Present	✓					
20	0	1.2	Normal*	Normal†	Present		✓				
30	0	1.2	Normal*	Normal†	Present		✓				
55	1	1.0‖	Extinguished	Blurred	Present				✓		
53	2	0.7	Extinguished	Blurred	Present				✓		
21	3	0.5	Extinguished	Blurred¶	Present			✓			
50	3	0.4	Extinguished	Blurred	Present				✓		
42	4	0.15	Extinguished	Blurred	Present				✓		
56	6	0.2	Extinguished	Blurred	Present				✓		
15	6	0.6	Extinguished	Blurred¶	Present			✓			
43	6	0.2	Extinguished	Blurred	Absent					✓	
9	7	0.5	Extinguished	Blurred	Present				✓		
27	7	0.4	Extinguished	Blurred	Present				✓		
61	7	0.2	Extinguished	Blurred	Present				✓		
35	7	0.3	Extinguished	Blurred	Present				✓		
10	8	0.5	Extinguished	Blurred¶	Present			✓			
13	8	0.1	Extinguished	Blurred	Present				✓		
19	8	0.15	Extinguished	Blurred	Present				✓		
24	8	0.5	Extinguished	Blurred	Present				✓		
45	8	0.2	Extinguished	Blurred	Absent					✓	
40	9	0.3	Extinguished	Blurred	Present				✓		
49	9	0.2	Extinguished	Blurred	Present				✓		
54	10	0.6	Extinguished	Blurred	Present				✓		
11	10	0.2	Extinguished	Blurred	Present				✓		
12	10	0.15	Extinguished	Blurred	Present				✓		
51	10	0.1	Extinguished	Blurred	Present				✓		
41	10	0.1	Extinguished	Blurred	Present				✓		
6	11	0.3	Extinguished	Blurred	Present				✓		
33	12	0.15	Extinguished	Blurred	Present				✓		
17	13	0.15	Extinguished	Blurred	Present				✓		
5	14	0.1	Extinguished	Blurred	Absent					✓	
1	15	0.2	Extinguished	Blurred	Present				✓		
25	15	0.3	Extinguished	Blurred	Present				✓		
57	15	0.3	Extinguished	Blurred	Absent					✓	
46	16	0.3	Extinguished	Blurred	Present				✓		
60	17	0.4	Extinguished	Blurred	Present				✓		
8	17	0.2	Extinguished	Blurred	Present				✓		
26	18	0.1	Extinguished	Blurred	Present				✓		
2	20	0.1	Extinguished	Blurred	Present				✓		
47	20	0.5	Extinguished	Blurred	Present				✓		
31	21	0.1	Extinguished	Blurred	Present				✓		
4	23	0.1	Extinguished	Blurred	Present				✓		
22	23	0.5	Extinguished	Blurred	Present				✓		
14	26	0.15	Extinguished	Blurred	Absent					✓	
48	29	0.15	Extinguished	Blurred	Present				✓		
52	29	0.3	Extinguished	Blurred	Absent					✓	
39	30	0.1	Extinguished	Blurred	Absent					✓	
59	37	0.3	Extinguished	Blurred	Absent					✓	
44	40	0.1	Extinguished	Blurred	Absent					✓	
23	49	0.1	Extinguished	Disrupted	Absent						✓
32	49	0.2	Extinguished	Blurred	Absent					✓	
37	49	0.3	Extinguished	Blurred	Present				✓		
38	53	0.2	Extinguished	Blurred	Present				✓		
7	59	0.08	Extinguished	Blurred	Absent					✓	
34	64	0.15	Extinguished	Disrupted	Absent						✓
2	65	0.2	Extinguished	Blurred	Absent					✓	
58	67	0.15	Extinguished	Disrupted	Absent						✓

* IZ, extinguished at the parafovea.
† EZ, blurred at the parafovea.
‡ IZ, minimal blurring at the foveal center.
§ EZ, minimal blurring at the foveal center.
‖ This patient complained of decreased vision although BCVA was 1.0.
¶ EZ, blurred only at the fovea.

Investigative Ophthalmology & Visual Science

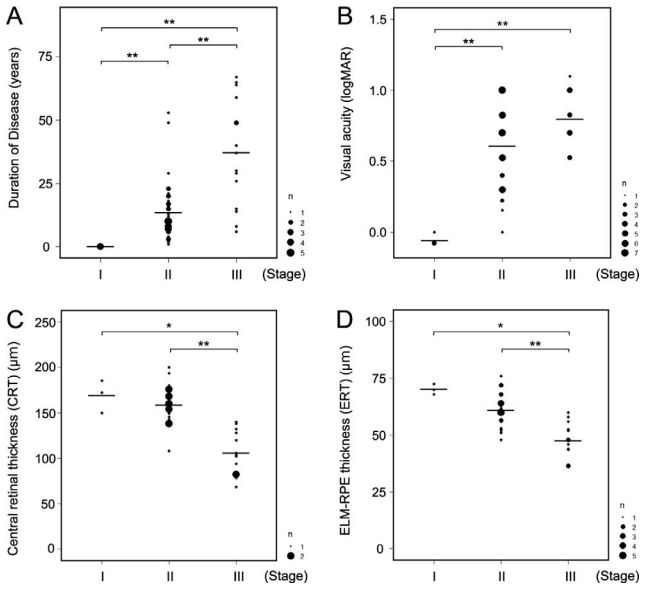

Figure 6. Comparison of disease duration, visual acuity, CRT, and ERT among three stages. The duration of the disease was significantly different between stages I and II (Steel-Dwass test; $P < 0.01$), between stages II and III ($P < 0.01$), and between stages I and III ($P < 0.01$) (**A**). The visual acuity was significantly different between stages I and II ($P < 0.01$), and between stages I and III ($P < 0.01$), but not between stages II and III ($P = 0.07$) (**B**). The CRT was significantly different between stages II and III ($P < 0.01$), and between stages I and III ($P < 0.05$), but not between stages I and II ($P = 0.64$) (**C**). ERT thickness at the foveola was significantly different between stages II and III ($P < 0.01$), and between stages I and III ($P < 0.05$), but not between stages I and II ($P = 0.07$) (**D**). (*$P < 0.05$, **$P < 0.01$).

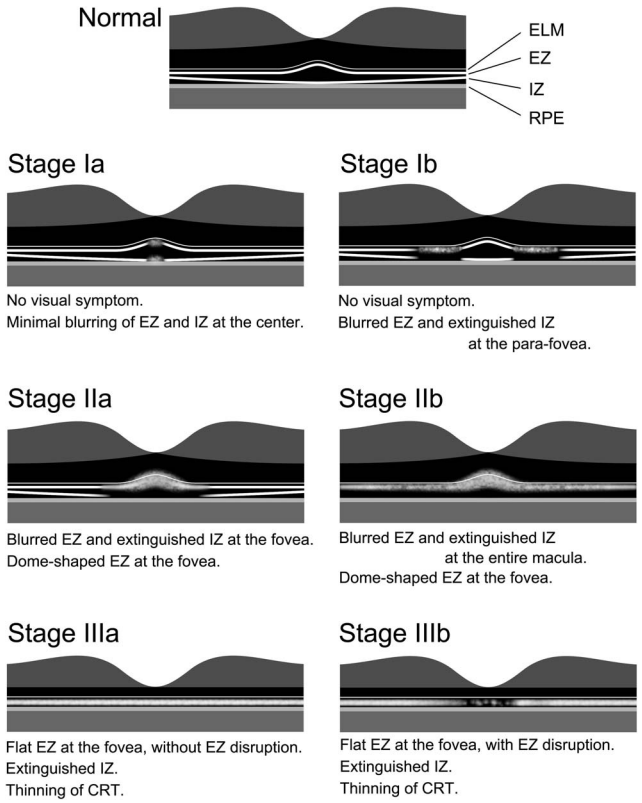

Figure 7. Schematic drawing of the clinical stages of occult macular dystrophy. Definition of the stage is shown below each drawing.

of the patients had a reduction of the foveal thickness to 75% of the normal average CRT and ERT was 29 years and 16 years, respectively (Figs. 5B, 5C). The difference between CRT and ERT indicated that the reduction of ERT preceded that of CRT during the course of OMD, and the changes in the thickness of photoreceptor layer may be more closely related to the decrease in the BCVA than in the total foveal thickness.

Similar patterns of disease progression have been reported for other diseases. In *ABCA4*-related retinopathy, Cideciyan et al.[18] measured the rod and cone photoreceptor–mediated vision serially and found a common underlying function of the progression of the disease; a normal plateau phase of variable length was followed by the initiation of retina-wide disease that progressed exponentially. Heeren et al.[19] investigated the expansion rate of macular telangiectasia (MacTel) type 2 after the onset of a scotoma, and they reported a common disease progression with little influence of the age when an absolute scotoma developed. These studies indicated that the course of the disease after the onset can be specific to the etiology of diseases, and predicting the disease course of individual patients will be valuable with regard to when to begin the treatments.

Stages of OMD

We have proposed that OMD can be divided into three clinical stages from I to III according to the photoreceptor structures in the OCT images (Tables 2, 3; Fig. 1). The grading was based on the fact that the IZ and EZ are vulnerable OCT markers in patients with OMD.[5,16] We have compared the disease duration, BCVA, CRT, and ERT among the three stages by Steel-Dwass tests (Fig. 6). The duration of the disease was significantly different between stages I and II ($P < 0.01$), stages II and III ($P < 0.01$), and stages I and III ($P < 0.01$; Fig. 6A). These results indicate that the three stages are associated with the duration of OMD although there was some overlap between stages II and III. The visual acuity was significantly different between stages I and II ($P < 0.01$), and between stages I and III ($P < 0.01$), but not between stages II and III ($P = 0.07$; Fig. 6B). These results indicate that visual acuity becomes progressively worse during the initial 15 years after onset but then becomes stable in the later years. The CRT was significantly different between stages II and III ($P < 0.01$) and between stages I and III ($P < 0.05$), but not between stages I and II ($P = 0.64$; Fig. 6C). These results indicate that the CRT does not change during the early stage but becomes progressively thinner in the later stages. The ERT was significantly different between stages II and III ($P < 0.01$) and between stages I and III ($P < 0.05$), but not between stages I and II ($P = 0.07$; Fig. 6D). These results are similar to those for CRT and indicate that the distance between the ELM and RPE does not change during the early stages but becomes progressively less in the later stages.

Although the stages in our cohort appeared to be related to the duration of the disease, there was considerable overlap in the duration and BCVA among the different stages (Table 3; Figs. 6A, 6B). This is because our staging was determined based on the structural changes in the OCT images but the age of onset was based on patients' report and did not necessarily reflect the actual age of onset. OMD is a very slowly progressive disease, and there should be cases that cannot be specifically defined to be at one stage. In applying this clinical staging, we propose that some cases can be classified as stage IIb or IIIa when the case has a partially preserved dome-shaped appearance of the foveal EZ.

A schematic drawing of the stages is shown in Figure 7. Stage I is a preclinical stage of OMD. The changes in the retinal

structure are minimal and the patients do not have any symptoms, but some patients had subtle abnormalities in the visual field tests. We suggest that stage Ia is the initial period for most OMD patients, and the blurring of the EZ and IZ will become apparent and gradually expand over the entire fovea and lead to stage IIa. On the other hand, stage Ib is a very unusual form of OMD.[16] Patients at stage Ib have good vision because both the EZ and IZ are preserved at the foveal center (Fig. 1). A sparing of the fovea is commonly observed in different types of macular diseases. Explanations for the physiological and anatomical sparing of the fovea have been presented in many publications,[20–28] but the mechanisms underlying central foveal sparing in OMD may be different from that of other disorders that typically have concurrent atrophy of the photoreceptors and the RPE.

Stage II was the largest group of OMD patients. Patients at stage IIa have photoreceptor abnormalities only at the fovea, and the impaired region gradually expands to the periphery leading to stage IIb, which has abnormalities in the entire macular region.

Stage III is the late stage of OMD. Patients at stage III have reduced CRT, and the foveal EZ is flat rather than dome-shaped. Patients at stage IIIa have a continuous EZ, but the foveal EZ will become disrupted, leading to stage IIIb. It is notable that even in the last stage, the structure of the RPE is normally preserved and an atrophic region could not be observed in any case either by OCT or by fundus autofluorescence (FAF).[5,29] The survival curve indicated that over 80% of patients can be predicted to retain a thickness of 50% of normal CRT and ERT for 60 years after the onset of symptoms (Figs. 5B, 5C). This indicates that the photoreceptor layer never becomes entirely atrophic as in other macular dystrophies such as Stargardt disease and achromatopsias.[13,30–32] The normally preserved RPE and partially preserved photoreceptor layer even in the late stage are the most essential characteristics of OMD. This preservation accounts for the fact that almost all patients with OMD are able to read large letters even in the late stage.

The *RP1L1* gene is believed to play important roles in the morphogenesis of the photoreceptors although the exact expression site within the photoreceptor has not been determined.[4] Cellular dysfunction due to an *RP1L1* mutation affects the photoreceptors, which becomes apparent first as an abnormality of both the IZ and EZ in OCT images. The preservation of the RPE may be partly due to partial preservation of the photoreceptor layer even at the late stage (Figs. 5B, 5C). However, further investigations on the function of RP1L1 protein are needed to determine the exact mechanisms that lead to the preservation of the RPE in cases of OMD.

Limitations

First, the age of onset was based on personal reports. OMD is a very slowly progressive disease, and the exact age of onset was difficult to determine accurately. This may be one reason why some patients (patients 43 and 45) with short disease durations were graded at stage III (Table 3).

Secondly, although we followed 29 patients for over 5 years, we could not observe any patients who converted their clinical stage during the follow-up period because OMD is very slowly progressive. Longitudinal follow-up OCT examinations over 20 years will be needed to further confirm the clinical stages of this disease.

In conclusion, we have determined the course of the OMD disease process in detail in the largest multicenter cohort, and we propose the clinical stages of OMD based on visual symptoms and OCT findings. The severity of disease stages is well correlated with the natural course of this disorder. We believe that the proposed stages will facilitate investigation of the pathogenicity of this disease and may provide important information for therapeutic strategies in treating OMD.

Acknowledgments

The authors thank the patients and their families for participation in this study. We thank Duco Hamasaki of the Bascom Palmer Eye Institute, University of Miami School of Medicine, Miami, Florida, for critical discussions and editing our manuscript.

Supported by research grants from the Japan Agency for Medical Research and Development (AMED), the Ministry of Health, Labor and Welfare, Japan (18ek0109282h0002, TI), Grants-in-Aid for Scientific Research, Japan Society for the Promotion of Science (H26-26462674, KT; 16H06269; 16KK0193, KF), and National Hospital Organization Network Research Fund (H30-NHO-Sensory Organs-03, KF, KT). Also supported by Foundation Fighting Blindness, USA, and Great Britain Sasakawa Foundation Butterfield Awards, UK (KF). The authors alone are responsible for the content and writing of the paper.

Disclosure: **N. Nakamura**, None; **K. Tsunoda**, None; **Y. Mizuno**, None; **T. Usui**, None; **T. Hatase**, None; **S. Ueno**, None; **K. Kuniyoshi**, None; **T. Hayashi**, None; **S. Katagiri**, None; **M. Kondo**, None; **S. Kameya**, None; **K. Yoshitake**, None; **K. Fujinami**, None; **T. Iwata**, None; **Y. Miyake**, None

References

1. Miyake Y, Ichikawa K, Shiose Y, Kawase Y. Hereditary macular dystrophy without visible fundus abnormality. *Am J Ophthalmol*. 1989;108:292–299.
2. Miyake Y, Horiguchi M, Tomita N, et al. Occult macular dystrophy. *Am J Ophthalmol*. 1996;122:644–653.
3. Miyake Y, Tsunoda K. Occult macular dystrophy. *Jpn J Ophthalmol*. 2015;59:71–80.
4. Akahori M, Tsunoda K, Miyake Y, et al. Dominant mutations in RP1L1 are responsible for occult macular dystrophy. *Am J Hum Genet*. 2010;87:424–429.
5. Tsunoda K, Usui T, Hatase T, et al. Clinical characteristics of occult macular dystrophy in family with mutation of RP1L1 gene. *Retina*. 2012;32:1135–1147.
6. Kabuto T, Takahashi H, Goto-Fukuura Y, et al. A new mutation in the RP1L1 gene in a patient with occult macular dystrophy associated with a depolarizing pattern of focal macular electroretinograms. *Mol Vis*. 2012;18:1031–1039.
7. Hayashi T, Gekka T, Kozaki K, et al. Autosomal dominant occult macular dystrophy with an RP1L1 mutation (R45W). *Optom Vis Sci*. 2012;89:684–691.
8. Ahn SJ, Cho SI, Ahn J, Park SS, Park KH, Woo SJ. Clinical and genetic characteristics of Korean occult macular dystrophy patients. *Invest Ophthalmol Vis Sci*. 2013;54:4856–4863.
9. Ziccardi L, Giannini D, Lombardo G, et al. Multimodal approach to monitoring and investigating cone structure and function in an inherited macular dystrophy. *Am J Ophthalmol*. 2015;160:301–312.
10. Davidson AE, Sergouniotis PI, Mackay DS, et al. RP1L1 variants are associated with a spectrum of inherited retinal diseases including retinitis pigmentosa and occult macular dystrophy. *Hum Mutat*. 2013;34:506–514.
11. Fujinami K, Kameya S, Kikuchi S, et al. Novel RP1L1 variants and genotype-photoreceptor microstructural phenotype associations in cohort of Japanese patients with occult macular dystrophy. *Invest Ophthalmol Vis Sci*. 2016;57:4837–4846.
12. Zobor D, Zobor G, Hipp S, et al. Phenotype variations caused by mutations in the RP1L1 gene in a large mainly German cohort. *Invest Ophthalmol Vis Sci*. 2018;59:3041–3052.
13. Greenberg JP, Sherman J, Zweifel SA, et al. Spectral-domain optical coherence tomography staging and autofluorescence

imaging in achromatopsia. *JAMA Ophthalmol*. 2014;132:437–445.

14. Lambertus S, Lindner M, Bax NM, et al. Progression of late-onset Stargardt disease. *Invest Ophthalmol Vis Sci*. 2016;57:5186–5191.
15. Ahn SJ, Ahn J, Park KH, Woo SJ. Multimodal imaging of occult macular dystrophy. *JAMA Ophthalmol*. 2013;131:880–890.
16. Kato Y, Hanazono G, Fujinami K, et al. Parafoveal photoreceptor abnormalities in asymptomatic patients with RP1L1 mutations in families with occult macular dystrophy. *Invest Ophthalmol Vis Sci*. 2017;58:6020–6029.
17. Fujinami K, Yang L, Joo K, et al. Clinical and genetic characteristics of East Asian patients with occult macular dystrophy (Miyake disease): East Asia Occult Macular Dystrophy Studies report number 1. *Ophthalmology*. 2019;126:1432–1444.
18. Cideciyan AV, Swider M, Aleman TS, et al. ABCA4 disease progression and a proposed strategy for gene therapy. *Hum Mol Genet*. 2009;18:931–941.
19. Heeren TF, Clemons T, Scholl HP, Bird AC, Holz FG, Charbel Issa P. Progression of vision loss in macular telangiectasia type 2. *Invest Ophthalmol Vis Sci*. 2015;56:3905–3912.
20. Chucair AJ, Rotstein NP, Sangiovanni JP, During A, Chew EY, Politi LE. Lutein and zeaxanthin protect photoreceptors from apoptosis induced by oxidative stress: relation with docosahexaenoic acid. *Invest Ophthalmol Vis Sci*. 2007;48:5168–5177.
21. Aleman TS, Cideciyan AV, Windsor EA, et al. Macular pigment and lutein supplementation in ABCA4-associated retinal degenerations. *Invest Ophthalmol Vis Sci*. 2007;48:1319–1329.
22. Curcio CA, Sloan KR Jr, Packer O, Hendrickson AE, Kalina RE. Distribution of cones in human and monkey retina: individual variability and radial asymmetry. *Science*. 1987;236:579–582.
23. Wang JS, Kefalov VJ. The cone-specific visual cycle. *Prog Retin Eye Res*. 2011;30:115–128.
24. Curcio CA, Millican CL, Allen KA, Kalina RE. Aging of the human photoreceptor mosaic: evidence for selective vulnerability of rods in central retina. *Invest Ophthalmol Vis Sci*. 1993;34:3278–3296.
25. Curcio CA, Allen KA, Sloan KR, et al. Distribution and morphology of human cone photoreceptors stained with anti-blue opsin. *J Comp Neurol*. 1991;312:610–624.
26. Okano K, Maeda A, Chen Y, et al. Retinal cone and rod photoreceptor cells exhibit differential susceptibility to light-induced damage. *J Neurochem*. 2012;121:146–156.
27. Snodderly DM, Sandstrom MM, Leung IY, Zucker CL, Neuringer M. Retinal pigment epithelial cell distribution in central retina of rhesus monkeys. *Invest Ophthalmol Vis Sci*. 2002;43:2815–2818.
28. Leveillard T, Mohand-Said S, Lorentz O, et al. Identification and characterization of rod-derived cone viability factor. *Nat Genet*. 2004;36:755–759.
29. Fujinami K, Tsunoda K, Hanazono G, Shinoda K, Ohde H, Miyake Y. Fundus autofluorescence in autosomal dominant occult macular dystrophy. *Arch Ophthalmol*. 2011;129:597–602.
30. Hirji N, Georgiou M, Kalitzeos A, et al. Longitudinal assessment of retinal structure in achromatopsia patients with long-term follow-up. *Invest Ophthalmol Vis Sci*. 2018;59:5735–5744.
31. Duncker T, Marsiglia M, Lee W, et al. Correlations among near-infrared and short-wavelength autofluorescence and spectral-domain optical coherence tomography in recessive Stargardt disease. *Invest Ophthalmol Vis Sci*. 2014;55:8134–8143.
32. Khan KN, Kasilian M, Mahroo OAR, et al. Early patterns of macular degeneration in ABCA4-associated retinopathy. *Ophthalmology*. 2018;125:735–746.

Investigative Ophthalmology & Visual Science